

A Novel Complex, RUNX1-MYEF2, Represses Hematopoietic Genes in Erythroid Cells

Boet van Riel,^a Tibor Pakozdi,^c Rutger Brouwer,^b Rui Monteiro,^f Kapil Tuladhar,^f Vedran Franke,^c Jan Christian Bryne,^c Ruud Jorna,^a Erik-Jan Rijkers,^b Wilfred van Ijcken,^b Charlotte Andrieu-Soler,^a Jeroen Demmers,^d Roger Patient,^f Eric Soler,^{a,d} Boris Lenhard,^{c,g} and Frank Grosveld^{a,d,e}

Department of Cell Biology and Center for Biomedical Genetics^a and Biomics Department,^b Erasmus Medical Center, Rotterdam, Netherlands; Computational Biology Unit-Bergen Center for Computational Science and Sars Centre for Marine Molecular Biology, University of Bergen, Bergen, Norway^c; Cancer Genomics Center^d and Center for Biomedical Genetics, Rotterdam, Netherlands^e; Molecular Hematology Unit, Weatherall Institute of Molecular Medicine, University of Oxford and John Radcliffe Hospital, Headington, Oxford, United Kingdom^f; and Department of Molecular Sciences, Institute of Clinical Sciences, Faculty of Medicine, Imperial College London, and MRC Clinical Sciences Centre, Hammersmith Hospital Campus, London, United Kingdom^g

RUNX1 is known to be an essential transcription factor for generating hematopoietic stem cells (HSC), but much less is known about its role in the downstream process of hematopoietic differentiation. RUNX1 has been shown to be part of a large transcription factor complex, together with LDB1, GATA1, TAL1, and ETO2 (N. Meier et al., *Development* 133:4913–4923, 2006) in erythroid cells. We used a tagging strategy to show that RUNX1 interacts with two novel protein partners, LSD1 and MYEF2, in erythroid cells. MYEF2 is bound in undifferentiated cells and is lost upon differentiation, whereas LSD1 is bound in differentiated cells. Chromatin immunoprecipitation followed by sequencing (ChIP-seq) and microarray expression analysis were used to show that RUNX1 binds approximately 9,000 target sites in erythroid cells and is primarily active in the undifferentiated state. Functional analysis shows that a subset of the target genes is suppressed by RUNX1 via the newly identified partner MYEF2. Knockdown of *Myef2* expression in developing zebrafish results in a reduced number of HSC.

The transcription factor RUNX1 (Aml1 or Cbfa2) is known to be important for the development of the hematopoietic system in mammals. It is part of a small family of core binding transcription factors with RUNX2 (Aml3 or Cbfa1), RUNX3 (Aml2 or Cbfa3) and CBF β . RUNX1 was first discovered as a homologue of the *Drosophila* segmentation gene *runt*. The RUNX1 protein binds DNA at the consensus sequence (TC)G(TC)GGT(TC) (3, 7). Several studies have shown that RUNX1 is important for the emergence of hematopoietic stem cells (HSC). The *Runx1* knockout (KO) mouse does not develop the definitive hematopoietic system (29, 33, 50) and has minor defects in the primitive hematopoietic system (57). The RUNX proteins form a heterodimer with CBF β that enhances the binding to DNA. This dimerization is important for the function of RUNX1, which is confirmed by the Cbf β KO mouse also lacking definitive hematopoietic development (39, 51).

It is known that RUNX1 has an important function in the development of macrophages (18) and megakaryocytes (9, 14, 35, 47, 56) after the emergence of the definitive HSC, but very little is known about its role in other lineages. A conditional knockout shows, however, some defect in the differentiation of erythrocytes. In one model, erythrocytes show a significantly higher number of Howell-Jolly bodies probably resulting from hyposplenism (36). Another model showed an increase in the ratio of maturing myeloid to erythroid cells compared to controls (15). A recent study has shown that RUNX1 is also important in primitive erythropoiesis (57). Defects were found in the morphology and Ter119 expression of primitive erythrocytes lacking RUNX1. Finally, RUNX1 homologues are also required for definitive erythropoiesis in nonmammalian vertebrates (21, 48). However, none of these studies shed much light on the molecular function of RUNX1. It is known that RUNX1 forms a repressive complex with mSIN3a in hematopoietic stem and progenitor cells (41) and in macrophages

(18), but nothing is known about the complex(es) it forms at later stages of differentiation.

Here we characterized the function of RUNX1 in adult erythropoiesis. RUNX1 was found to be present in a complex containing essential regulators of erythropoiesis such as LDB1, GATA1, and TAL1 (24). Next, novel protein partners and target genes were identified using mass spectrometry and chromatin immunoprecipitation followed by sequencing (ChIP-seq). A number of these RUNX1 target genes are important for erythropoiesis, and we show that RUNX1 regulates these genes via MYEF2, a repressor previously unknown to be active during erythropoiesis. Importantly, morpholino knockdown of *Myef2* or *Runx1* in zebrafish results in reduced numbers of HSC, suggesting that these two factors also interact *in vivo* to regulate hematopoiesis.

MATERIALS AND METHODS

Tagging *Runx1* construct. An NheI restriction site was inserted into the cDNA of the large *Runx1* isoform to remove the first ATG and allow insertion of the tag. The Bio-V5 double tag was ligated into the NheI site to create N-terminally tagged *Runx1* cDNA (2, 8, 23, 43). The tagged *Runx1* cDNA was cloned into the NotI site of a *Gata1* promoter-based expression vector (28, 34, 46).

Cell culture. Mouse erythroleukemia (MEL) cells were cultured in Dulbecco modified Eagle medium containing 10% fetal calf serum and

Received 14 July 2011 Returned for modification 6 August 2011

Accepted 8 July 2012

Published ahead of print 16 July 2012

Address correspondence to Frank Grosveld, f.grosveld@erasmusmc.nl, or Boris Lenhard, b.lenhard@csc.mrc.ac.uk.

Copyright © 2012, American Society for Microbiology. All Rights Reserved.

doi:10.1128/MCB.05938-11

1% penicillin-streptomycin. The addition of 2% dimethyl sulfoxide (DMSO) was used to induce erythroid differentiation. Cells were harvested after 4 days of differentiation.

Immunoprecipitations. N-terminally tagged *Runx1* cDNA was stably expressed in MEL cells containing the bacterial biotin ligase BirA (6). Nuclear extracts and immunoprecipitations (IPs) were prepared as described previously (6, 37, 43). Bio-V5-RUNX1 IPs from nuclear extracts were performed using V5 affinity agarose beads from Sigma. The antibodies used in the present study are listed elsewhere (<http://www.erasmusmc.nl/47738/185891/973174/3784765/mcb2012>). Washes were performed using HENG150 (150 mM KCl, 20 mM HEPES, 20% glycerol, 0.25 mM EDTA, 0.05% NP-40). IPs were performed in the presence of benzonase endonuclease to exclude the identification of complexes formed via DNA binding.

ChIP and ChIP-seq sample preparation. ChIP analyses were performed as described previously (23, 43–45). For ChIP 2×10^7 MEL cells and for ChIP-seq 1×10^7 MEL cells were used. The antibodies and primers used for ChIP are described in detail elsewhere (<http://www.erasmusmc.nl/47738/185891/973174/3784765/mcb2012>).

RNAi in MEL cells. The TRC Mission human and mouse library from Sigma was used for shRNA mediated knockdown of proteins of interest. They were delivered to MEL cells via lentiviral transduction. Virus was added to 0.5×10^6 MEL cells that were cultured for 48 h. Puromycin was added, and nuclear extracts and/or total RNA were prepared 48 h later. For induced MEL cells, DMSO was added to the medium, together with the puromycin, and the cells were harvested 4 days later.

Zebrafish morpholino injections. Fish were bred and maintained as described previously (26, 52) and staged as described previously (22). Morpholino-oligonucleotides (MOs; obtained from Gene Tools, LLC, Oregon) were designed to target splice junctions in the un-spliced *Myef2* mRNA. *Myef2* MO 5'-CTCACCACTACATGAGACATACAA-3', targeting the intron2-exon3 junction, affected the *Myef2* mRNA efficiently. Typically, 1 nl of *Myef2* MO (6.5 ng/nl) was injected into one- to two-cell-stage embryos. Uninjected zebrafish embryos were used as a wild-type control. The knockdown efficiency was verified by PCR using wild-type and MO-injected embryo cDNAs with the following gene-specific primers: *Myef2*-F (CAGAACCAAGACGACACGAA) and *Myef2*-R (CGATG GATGGAGGAATGTTT). Primers against the *ef1 α* gene (forward, GGC CACGTCGACTCCGAAAGTCC; reverse, CTCAAAACGAGCCTGGC TGTAAGG) were used as a loading control for the PCR. Uninjected zebrafish were used as a wild-type control.

Whole-mount *in situ* hybridization. Whole-mount *in situ* hybridization was carried out as described previously (20). Digoxigenin-labeled antisense RNA probes were transcribed from linearized templates using T3, T7, or Sp6 RNA polymerases (Roche, Burgess Hill, United Kingdom). After hybridization, the embryos were bleached as required in 5% formamide–0.5 \times SSC (1 \times SSC is 0.15 M NaCl plus 0.015 M sodium citrate)–10% H₂O₂ for 10 to 30 min, washed in PBST (phosphate-buffered saline, 0.1% Tween 20), and transferred to 80% glycerol for imaging.

Computational analysis of microarray and ChIP-seq data. The bioinformatics analysis and visualization of the microarray and ChIP-seq data were carried out as described previously (43, 44). Expression levels were normalized and fitted with Bayesian linear regression model for discovery of differentially expressed genes. The ChIP-seq data were filtered to correct for PCR bias, low sequencing quality, assignment to chromosomes of no interest, and nonunique mapping during the read alignment. Peaks were called for the continuous genomic regions of at least five reads (a false discovery rate [FDR] of <0.05) and having a fold change 5-fold higher than that of the control. The detected peaks were assigned to the closest genes, following the intersection of the two data sets, which was performed to ensure that genes taken for later analysis have been both differentially expressed and significantly enriched in two independent experiments (1, 19).

Accession numbers. ChIP data were deposited in the European Nucleotide Archive under accession no. ERP001491. RNAi data were deposited in the ArrayExpress repository under accession no. E-MTAB-1171.

RESULTS

Tagging *Runx1* and generating stable MEL cell lines. It was previously shown that RUNX1 interacts with the essential transcription factors TAL1 and LDB1 and binds overlapping sites genome-wide in hematopoietic cells (17, 24, 54). From those experiments it was not clear whether RUNX1 is an integral member of the complexes or a cooperating factor binding in close proximity to the LDB1 complex. We thought to resolve this question by determining first which genes or sequences are targeted by the RUNX1 protein. For this purpose and allowing the purification of complexes formed by RUNX1, a Bio-V5 tag was inserted at the N terminus at the 5' end of the *Runx1* cDNA starting from the initiation of translation site of the distal promoter (Fig. 1A). The cDNA was stably expressed in BirA-expressing MEL cells (6) using a *Gata1* promoter-based expression vector. Several clones were tested to avoid problems of overexpression artifacts, and clone 7 was chosen because it gave low Bio-V5-RUNX1 expression close to the endogenous levels (Fig. 1B). Clone 7 also grew normally under noninduced or induced (2% DMSO) tissue culture conditions compared to nontransfected MEL cells. Figure 1B also shows that the IP of Bio-V5-RUNX1 is efficient because it is almost absent in the supernatant of the IP.

Murine genome-wide RUNX1 DNA binding sites. The Bio-V5-tagged version of RUNX1 was subsequently used to identify the genome-wide DNA binding sites of RUNX1 by ChIP, followed by high-throughput sequencing (i.e., ChIP-seq). Surprisingly, biotinylation of Bio-V5-RUNX1 by BirA was inefficient (data not shown), and hence a V5 antibody was used for the ChIP analyses. The *Runx1* +23.5 enhancer was used as a positive control for the ChIP to show that the Bio-V5 tagged RUNX1 and endogenous RUNX1 were bound to this enhancer (30) (see also Fig. S1 at <http://www.erasmusmc.nl/47738/185891/973174/3784765/mcb2012>). A total of 13 million unique reads were mapped to the mouse genome, and the genome-wide binding sites were combined with microarray data of differentially expressed genes to show their distribution around genes up- and downregulated in differentiating MEL cells (44). Figure 2A shows the position of RUNX1 binding relative to the transcriptional start site (TSS) of differentially expressed genes on the *x* axis versus the fold expression change during erythroid differentiation on the *y* axis. All genes that have a RUNX1 peak in close proximity in MEL cells are shown in Tables S1 and S2 at the URL above. A Venn diagram with the overlap of RUNX1 binding sites in noninduced and induced MEL cells and hematopoietic progenitor cells can be found in the supplemental online data. This analysis shows that the majority of RUNX1 binding sites between induced and noninduced MEL cells are the same. The nonoverlap with the hematopoietic progenitor cells (54) is much larger, indicating that there is a very substantial difference in the number of targets (see Fig. S2A at the URL above).

The result shows that RUNX1 binds to a significant number of genes that are up or downregulated upon differentiation in non-induced and induced MEL cells, many of which are involved in erythroid differentiation, such as *Cbfa2t3* (Eto2), *Gata1*, and *Zfp1* (Fog1) (see Table S1 at <http://www.erasmusmc.nl/47738/185891/973174/3784765/mcb2012>). Induced cells show less

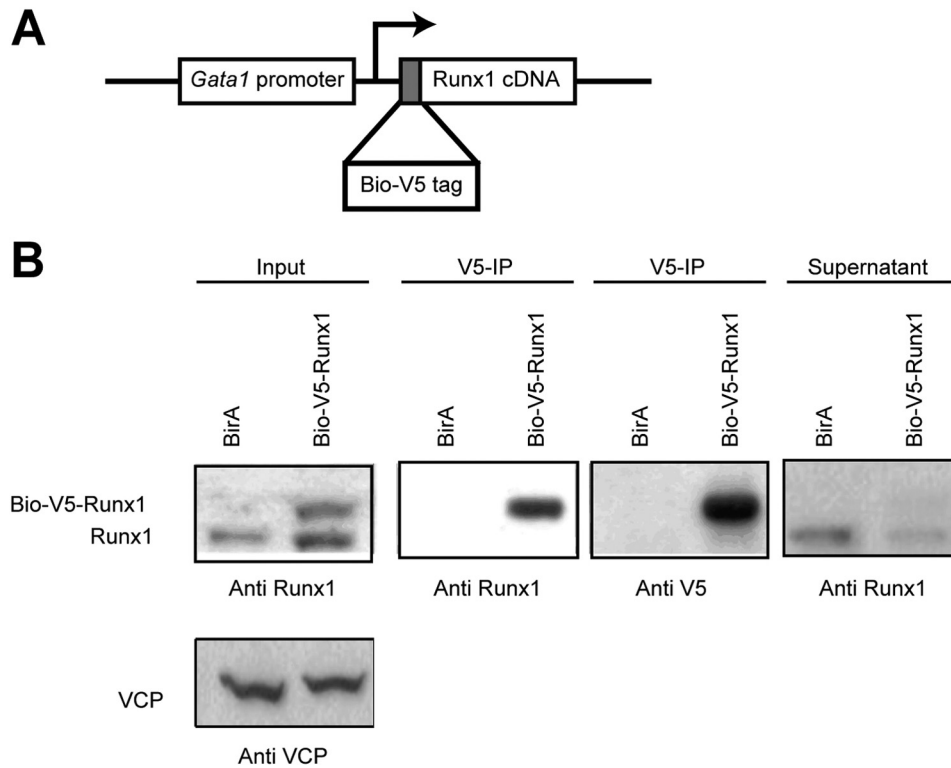


FIG 1 Bio-V5-RUNX1 and V5 IP. (A) Schematic view of Bio-V5-RUNX1. A Bio-V5 double tag was ligated onto the 5' end of the *Runx1* cDNA (long isoform, starting from the distal promoter) and cloned into a *Gata1*-based expression vector (46). (B) Expression of Bio-V5-RUNX1 in MEL cells clone 7 and compared to endogenous levels of RUNX1 in BirA control cells. The V5-IP was analyzed on Western blots with anti-RUNX1 or anti-V5 staining. The VCP protein was used as a loading control.

binding of RUNX1 to upregulated genes, although the overall binding pattern hardly changes (Fig. 2A).

A motif discovery analysis of 200 bp around RUNX1 binding peaks shows a GATA1 binding motif to be present at 74% of these peaks (Fig. 2B). Cooperative binding of RUNX1 and GATA1 was previously observed in megakaryocytes (35). A typical LDB1 complex binding motif composed of a GATA motif neighbored by a (partial) E-box (TAL1 binding) 7 to 8 bases upstream was found in 59% to be closely associated with RUNX1 binding sites. This confirms the original observation that RUNX1 associates with the GATA1/LDB1/TAL1 complex (24, 47). The overlap between RUNX1 and the GATA1/LDB1/TAL1 complex in noninduced and induced MEL cells is seen in Fig. S2 and Table S2 (<http://www.erasmusmc.nl/47738/185891/973174/3784765/mcb2012>).

RUNX1 binding to erythroid specific genes. To verify the binding to regulatory elements of important or typical hematopoietic genes, we checked binding to the genes *Gata1*, *Cbfa2t3* (Eto2), and *Epb4.2*. GATA1 is an important regulator of erythropoiesis and essential for terminal differentiation (reviewed in reference 4). ETO2 was shown to be part of the GATA1/LDB1/TAL1 complex in erythroid cells (11, 13, 24, 44), and its absence causes an erythroid phenotype in mice (5). Both the transcription factors *Gata1* and *Cbfa2t3* (Eto2) genes were top hits in the RUNX1 ChIP-seq data. Band 4.2 (*Epb4.2*) is a structural membrane protein of erythrocytes that is highly upregulated in differentiating erythroid cells (reviewed in reference 40).

RUNX1 binds to the promoter region of *Gata1*, *Cbfa2t3* (Eto2), and *Epb4.2* and to the upstream erythroid HS3.5 enhancer

of *Gata1* (Fig. 3). This binding is observed in both noninduced and induced MEL cells. No binding was observed in the negative controls, the 3' untranslated region (3'UTR) of the *Gata1* and *Epb4.2* genes, and 2 kb downstream of the *Cbfa2t3* (Eto2) promoter.

Figure S3 (<http://www.erasmusmc.nl/47738/185891/973174/3784765/mcb2012>) shows all of the RUNX1 binding sites and their sequences identified via ChIP-seq at the *Gata1*, *Cbfa2t3* (Eto2), and *Epb4.2* genes. Many of these sites are conserved in human megakaryocytes (47).

Knockdown of *Runx1* shows a function as both a transcriptional repressor or activator. In order to determine which of the genes found by ChIP-seq are real targets of RUNX1, five different *Runx1* shRNAs (shRunx1#1 to shRunx1#5) were tested in MEL cells. Western blots of nuclear extracts showed that only shRunx1#1 and shRunx1#2 transduction resulted in a partial knockdown (KD) of RUNX1 protein (see Fig. S4 at <http://www.erasmusmc.nl/47738/185891/973174/3784765/mcb2012>) and mRNA (Fig. 4A) in MEL cells versus the control shTRC. The genome-wide expression obtained by microarray analysis from *Runx1* KD in noninduced and induced MEL cells (see Tables S3 and S4 at the URL above) were then correlated to the RUNX1 ChIP-seq data to identify RUNX1 target genes (Fig. 5). The analysis before differentiation identified sets of genes that are up- or downregulated as a result of the RUNX1 KD, which suggests that RUNX1 can function both as an activator and repressor in erythroid cells. Figure 5 also shows that RUNX1 is usually not bound close to the TSS of potential target genes. Most of the RUNX1 repressed genes show only a moderate increase of expression

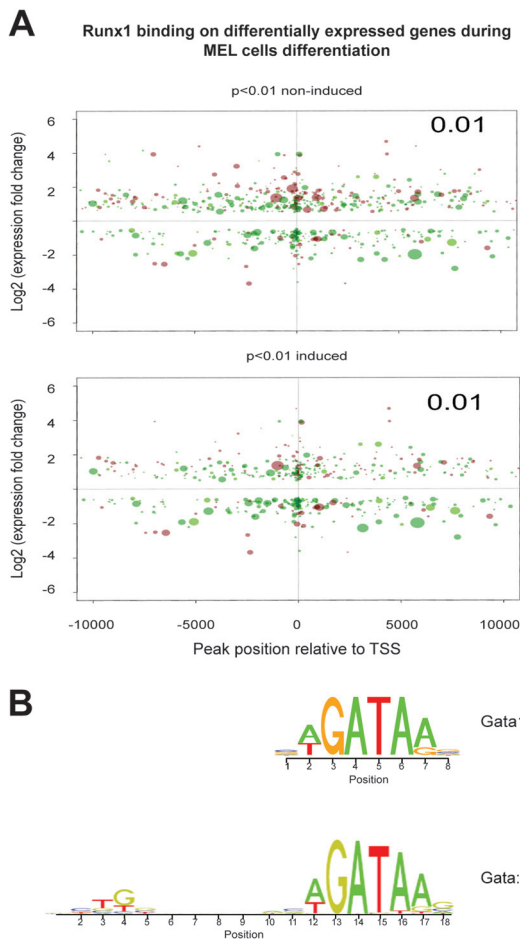


FIG 2 RUNX1 genome-wide binding patterns. (A) Bubble plot representation of RUNX1 ChIP-sequencing binding to differentially expressed genes during differentiation. Intersection between differentially expressed genes (FDR < 0.05) and ChIP-seq binding sites (FDR < $1e-10$) identifies the RUNX1 target genes. Four categories of information are shown with bubble plot: the relative distance of the closest TSS to the RUNX1 peak summits (x axis), the \log_2 expression of the fold change of the closest gene (y axis), the maximum read count at the bound region (bubble size), and the promoter overlap with the CpG island (color). Brown bubbles, gene TSS in non-CpG regions; green bubbles, gene TSS in CpG region. (B) Motif discovery analysis of 200 bp around RUNX1 binding sites. The GATA motif discovered ca. 74% of the RUNX1 binding site. Also, a GATA motif neighbored by an E-box (TAL1 binding) was frequently discovered around RUNX1 binding sites.

after the RUNX1 KD (e.g., *Cbfa2t3* [Eto2] and *Gata1* [Fig. 4A]), which is probably due to the fact that the KD is only partial. However, others, such as *Ebp4.2* (Fig. 4A), are very sensitive to the level of RUNX1 and show a dramatic increase in expression, suggesting that RUNX1 is a major repressor of such genes in undifferentiated cells. In differentiated cells much fewer genes are affected and to a lower extent, which correlates with a decrease of RUNX1 binding. A number of the genes that are suppressed by RUNX1 in the undifferentiated cells are part of different signal transduction pathways that involve the coreceptor CSF2RB affecting interleukin-3 (IL-3), IL-5, IL-9, and CSF2 signaling, and IL-9R, which are all involved in hematopoietic differentiation and, importantly, EpoR, required for red cell expansion (see Table S1 at <http://www.erasmusmc.nl/47738/185891/973174/3784765/mcb2012>). Several cell cycle regulators (e.g., p21 and cyclin E) are also suppressed

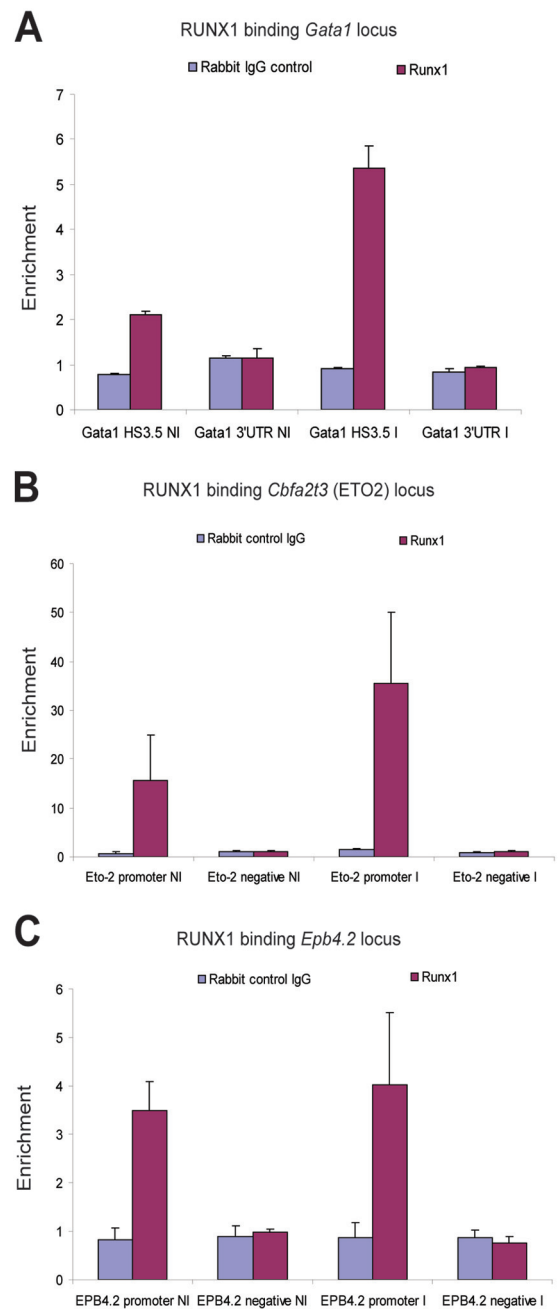


FIG 3 Confirmation of ChIP-seq results via endogenous RUNX1 ChIP. ChIPs were performed in noninduced (NI) and induced (I) MEL cells. Rabbit anti-RUNX1 and rabbit control IgG ChIPs are indicated in purple and blue, respectively. (A) ChIP enrichments obtained for the *Gata1* HS3.5 enhancer and a negative region at the *Gata1* gene 3'UTR. (B) ChIP enrichments at the *Cbfa2t3* (Eto2) promoter and negative region 2 kb downstream of TSS. (C) ChIP enrichments at the *Epb4.2* promoter and negative region (*Epb4.2* gene 3'UTR).

by RUNX1. We therefore conclude that RUNX1 plays an important role in erythroid development up to the final differentiation steps. Interestingly, NF- κ B, which regulates among other processes proliferation and apoptosis, is positively regulated by RUNX1.

Our previous results show that the GATA1/TAL1/LDB1 complex acts mainly as an activator in late erythroid differentiation.

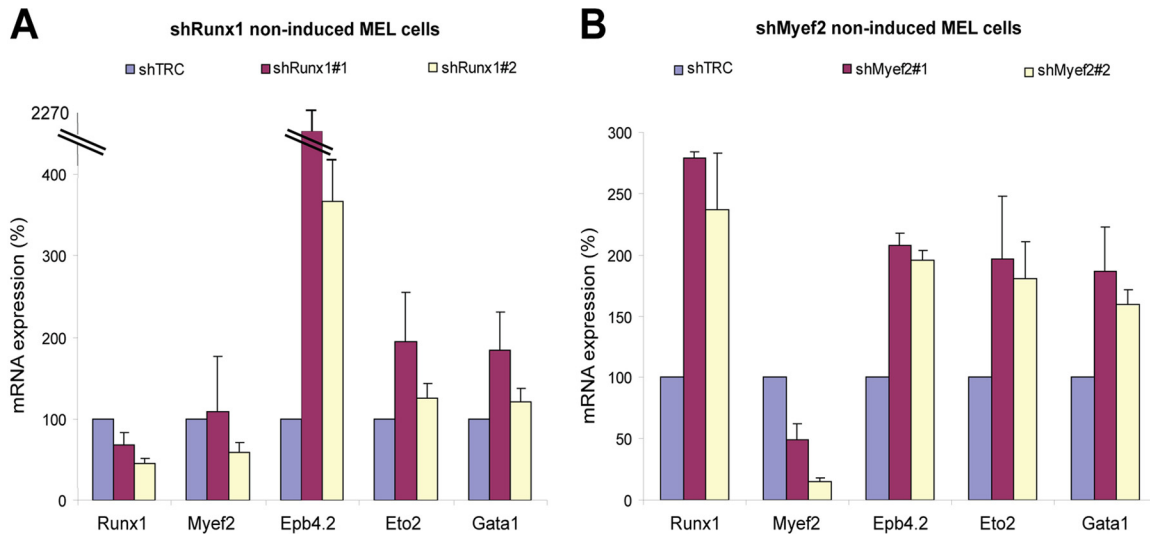


FIG 4 Effects of knockdown of *Runx1* and *Myef2*. Expression levels were measured by qPCR for *Runx1*, *Myef2*, *Epb4.2*, *Cbfa2t3*, and *Gata1* mRNAs. (A) *Runx1* and (B) *Myef2* KD in noninduced MEL cells compared to the nontargeting shTRC control shRNA.

Recent data (E. Soler et al., unpublished data) show that this activation is primarily achieved through the release of repression in the differentiated cells. RUNX1 may be an important player in this regulation by suppression. The overlap in binding of RUNX1 with GATA1 and TAL1 binding is highest in genes repressed by RUNX1 (see Table 2), which is consistent with the role of the GATA1/TAL1/LDB1 complex in undifferentiated cells. We were therefore interested in determining whether RUNX1 binds any protein partners not found in the LDB1 complex that may have a repressive role.

Proteomics identification of RUNX1 protein partners. Single-step purifications of Bio-V5-RUNX1 complexes were used with V5-agarose beads and the resulting proteins analyzed by liquid chromatography-tandem mass spectrometry. Control V5-Immunoprecipitations were performed in BirA-MEL cells not containing the Bio-V5-RUNX1 vector. The mass spectrometry data (Table 1) show the proteins that were pulled down specifically in the Bio-V5-RUNX1-containing cells. As expected, a number of known RUNX1 partners were found such as CBF β , GATA1, ETO2, and TAL1 (9, 24, 31, 32, 56), confirming that the tagged RUNX1 forms the appropriate complexes and is indeed associated with the LDB1 complex in erythroid cells. However, a number of novel potentially repressing proteins or complexes were also identified, in particular LSD1, a histone-modifying enzyme, and MYEF2, a factor previously only described in myelinating cells (16).

The LSD1 complex was found to bind in differentiated cells only. It contains LSD1, GFI1b, and CoREST and has been shown to be important in hematopoiesis (17, 38). LSD1, the first histone demethylase identified in mammals, demethylates H3K4 to enable gene repression (10, 42). However, recent evidence showed that LSD1 can also function as an activator by demethylating H3K9 via an as-yet-unknown mechanism (12, 25, 55). The RUNX1-LSD1 interaction was validated by immunoprecipitations using antibodies against endogenous LSD1 (see Fig. S5 at <http://www.erasmusmc.nl/47738/185891/973174/3784765/mcb2012>) and confirmed that the proteins were mainly interacting in differentiating cells.

Myelin expression factor 2 (MYEF2) was a better potential repressor to function with RUNX1 in undifferentiated cells as it was mostly identified in undifferentiated cells (Table 1). This factor was not known to be expressed or to form complexes in hematopoietic cells and had previously only been identified as a repressor of the mouse myelin basic protein gene binding DNA directly (16). It contains two RNA recognition motifs (RRM) that have been shown to be responsible for binding to DNA (27). The binding of MYEF2 in undifferentiated cells was confirmed using the tagged RUNX1 protein (Fig. 6; see also Fig. S6 at <http://www.erasmusmc.nl/47738/185891/973174/3784765/mcb2012>). The binding of MYEF2 to endogenous RUNX1 using an antibody IP showed only a weak band, due to the poor quality of the antibody, which results in an inefficient RUNX1 endogenous IP. Alternatively, the antibody may interfere with the epitopes also recognized by MYEF2. The V5-IP shows that the RUNX1-MYEF2 complex is primarily present in noninduced MEL cells and almost absent in induced cells. The reverse IP for MYEF2 with the antibodies currently available failed, and we were unable to tag the N or C terminus of MYEF2 successfully. It should be noted that even though the IPs are all performed in the presence of benzonase, which cleaves DNA and RNA, it cannot be excluded that the interaction between MYEF2 and RUNX1 is facilitated via DNA.

Knockdown of *Myef2* mimics the knockdown of *Runx1*. Figure 4B shows that the two shRNA vectors against *Myef2* transcripts result in a KD of 50% or more in the undifferentiated MEL cells. This results in increased expression of the *Runx1*, *Cbfa2t3* (*Eto2*), and *Gata1* genes, suggesting that RUNX1 indeed represses these genes via MYEF2. However, the transcripts of *Epb4.2* were much less dramatically increased compared to the RUNX1 KD, confirming that factors other than MYEF2 are also important for the repression of this particular gene, e.g., *Cbfa2t3* (*Eto2*) KD gives a 6-fold upregulation of *Epb4.2* (44). We next thought to determine whether MYEF2 binds to the same sites as RUNX1; however, all available antibodies are not of ChIP-grade quality. As mentioned above, a tagging approach at the N or C terminus of MYEF2 also failed, suggesting that the termini are important for the struc-

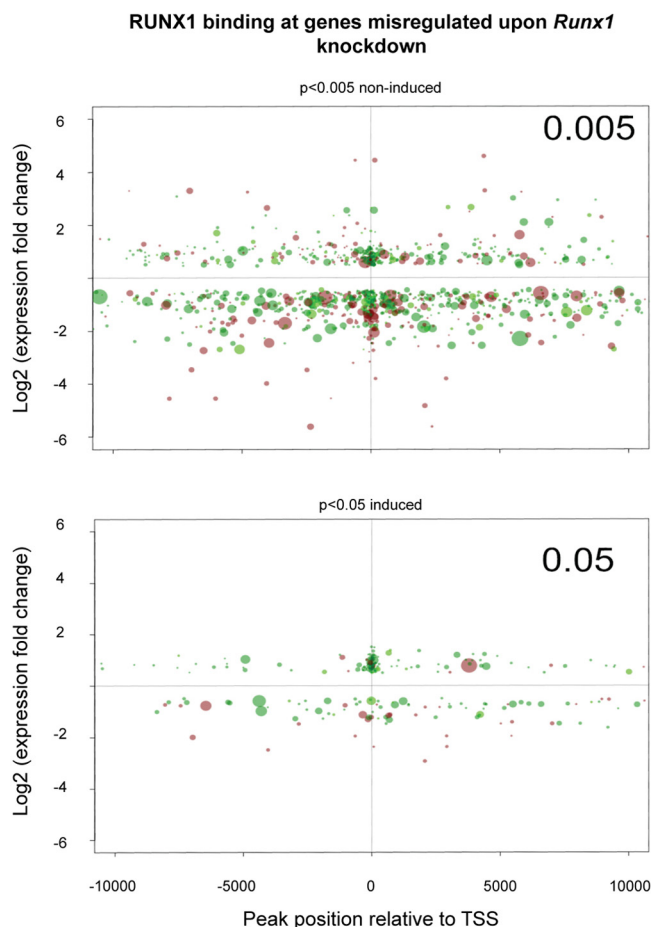


FIG 5 Genome-wide identification of RUNX1 target genes. Bubble plot representation of RUNX1 binding sites on genes differentially expressed in *Runx1* knockdown MEL cells (KD). False discovery rates (FDR) of <0.005 and <0.05 were applied for undifferentiated cells and differentiated cells, respectively. Each bubble represents a gene. The x axis shows the position of RUNX1 binding relative to the transcription start site (TSS). The y axis shows the \log_2 fold change in expression after *Runx1* KD. A negative log value therefore represents genes activated by RUNX1, whereas a positive value represents genes suppressed by RUNX1. The size of the bubble is proportional to the number of ChIP-seq reads (peak height), which is a relative measure of binding. Brown bubbles represent genes with promoters not overlapping CpG regions, and green bubbles represent bound genes with promoters overlapping CpG regions.

ture and/or stability of the protein. Nevertheless, we conclude that RUNX1 has a suppressive role before induction and that this role is mediated via MYEF2 because we frequently observed MYEF2 binding sites in association with RUNX1 binding sites (see Fig. S3A to C at <http://www.erasmusmc.nl/47738/185891/973174/3784765/mcb2012>). In order to at least test *in vitro* whether the two factors associate with an oligonucleotide from the *Gata1* HS3.5 enhancer was used to show that both RUNX1 and MYEF2 bind these sequences (see Fig. S7 at the URL above). When either the RUNX1 or the MYEF2 binding site is mutated the binding is lost, suggesting cooperative binding.

Myef2 morpholino injections in zebrafish show a hematopoietic phenotype. Factors associated with a complex in undifferentiated cells *in vitro* often already have a role much earlier in hematopoietic development (24). We therefore carried out *Myef2* knockdown experiments in zebrafish. *Myef2* MO was injected into

the zebrafish one-cell-stage embryos, which resulted in a *Myef2* knockdown. The *Myef2* MO induces missplicing of the intron2-exon3 junction, as shown by the appearance of an extra band in the PCR analysis of *Myef2* morphant cDNA and a reduction in the wild-type band (Fig. 7A). This extra band is misspliced mRNA lacking exon 3 and containing a frameshift mutation that is not translated into functional protein, thus knocking down *Myef2*.

mRNA levels of a number of hematopoietic genes expressed in developing zebrafish were visualized by *in situ* hybridization. *Runx1* and *Gata1* mRNA were assessed 20 h postfertilization (hpf), which is the period of time that the primitive hematopoietic system develops. Figure 7B shows that the levels of *Gata1* and *Runx1* mRNA are unchanged in the primitive hematopoietic system in the MO-injected zebrafish compared to the wild type. However, a clear defect in definitive hematopoiesis is observed at later stages by a decreased expression of *Runx1* (Fig. 7C). To determine whether this downregulation corresponded to a decrease in HSC and their derivatives, we analyzed the expression of *cMyb* and *Gata1* in the CHT 4 days postfertilization (dpf), which mark HSC/definitive progenitors and definitive erythroid cells, respectively (Fig. 7C). The expression of both *cMyb* and *Gata1* was severely reduced in the CHT of *Myef2* morphants at 4 dpf. In addition, expression of Ikaros and Rag1 in the thymus indicative of the presence of HSC-derived T-cell progenitors (49, 53) was absent in *Myef2* morphants. Vascularization and the development of the pronephric duct is unaffected in the MO-injected zebrafish (data not shown). Taken together, these results indicated that *Myef2* is required for HSC emergence, probably as part of a complex that includes RUNX1. Furthermore, knockdown of MYEF2 partners in zebrafish also show a reduction in HSC (21; C. Andrieu-Soler et al., unpublished data).

DISCUSSION

RUNX1 is an essential regulator in the emergence of the HSC. However, the role of RUNX1 beyond HSC formation and maintenance in erythroid cells was poorly understood. In the present study, a previously unknown role of RUNX1 in erythropoiesis is uncovered by showing that it acts as a repressor of a number of erythroid genes via the repressor protein MYEF2. Using morpholinos in zebrafish, we show this factor to be of general importance in hematopoiesis.

TABLE 1 Mass spectrometry results for Bio-V5-RUNX1 V5 immunoprecipitation^a

Protein	C88/BirA	Bio-V5-RUNX1 noninduced	Bio-V5-RUNX1 induced
Core binding factors			
CBFB	–	+	+
ETO2	–	–	+
Hematopoietic proteins			
GATA1	–	+	+
TAL1	–	+	+
LSD1 complex			
LSD1	–	–	+
COREST1	–	–	+
GFI1B	–	–	+
GSE1 ^b	–	–	+
Repressor: MYEF2	–	+	+/-

^a –, no binding found; +, strong binding found; +/-, medium binding found.

^b GSE1, genetic suppressor element 1.

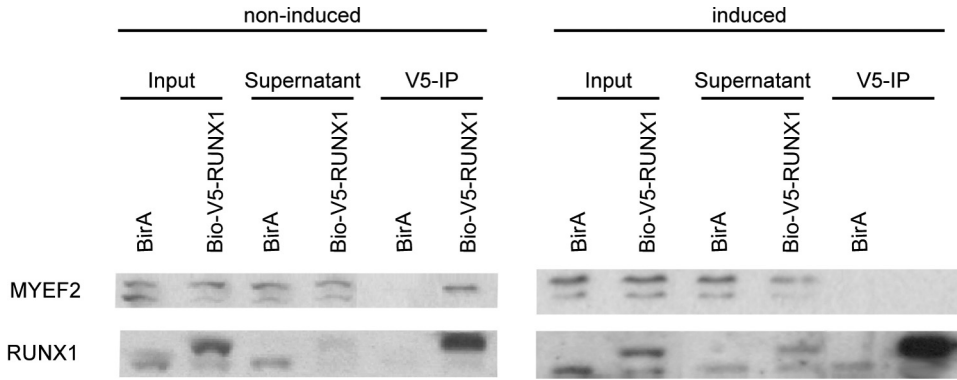
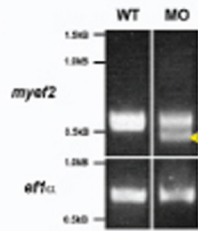


FIG 6 Validation of the mass spectrometry data using Bio-V5-RUNX1 IPs. Western blots of a V5 specific IP of Bio-V5-RUNX1 in noninduced and induced MEL cells. The V5 IP in nontransfected MEL cells was used as a control. RUNX1 and MYEF2 were detected by Western blotting and RUNX1 specific or MYEF2 specific immunostaining.

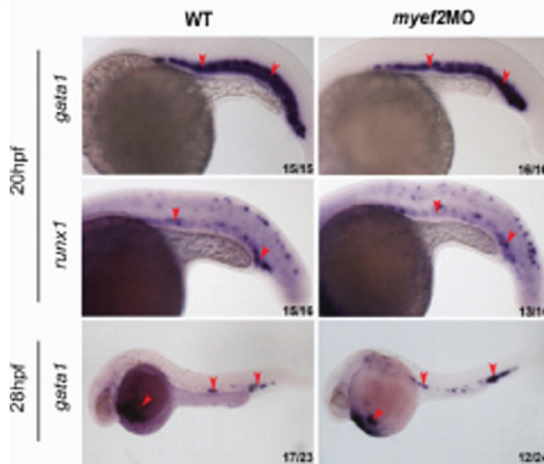
RUNX1 was recently shown to regulate corepressor interactions of PU.1 in macrophage differentiation (18). RUNX1 was already known to have a function in the development of megakaryocytes, which develop from the same progenitor cell as ery-

throid cells and where RUNX1 also functions as a repressor (reviewed in reference 14). The complex of RUNX1 and GATA1 has been described in megakaryocytes (9, 56), but it is not clear what function it has during megakaryocytic development and whether

A



B



C

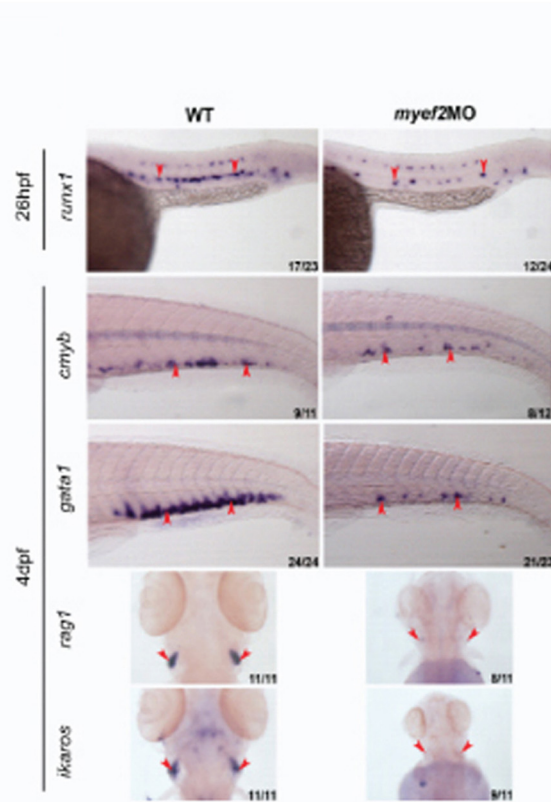


FIG 7 Zebrafish splice morpholino injections against zebrafish *Myef2*. (A) PCR on *myef2* and housekeeping gene *efl1α* cDNA. In MO injected zebrafish an extra PCR band is seen (yellow arrowhead) corresponding to a loss of exon three from *Myef2*. (B) Markers of primitive blood in the intermediate cell mass at 20 hpf. (C) Markers of definitive blood. At 26 hpf, *Runx1* marks emerging HSC in the dorsal aorta. At 4 dpf in the caudal hematopoietic tissue, *cMyb* marks HSC and their derivatives, and *Gata1* marks the erythroid population. *Rag1* and *Ikaros* mark thymic T cells.

a complex is formed with LSD1 or MYEF2. Two recent genome-wide studies again show the RUNX1-GATA1 complex to be important for megakaryocytic development (35, 47). It therefore appears that RUNX1 is not only important for the formation of stem cells but that it is an important suppressive regulatory factor in (a number of) the downstream myeloid cells.

The interaction of RUNX1 with LSD1 was confirmed in erythroid cells via co-IP with antibodies against RUNX1 and LSD1 in both noninduced and induced cells. However, the LSD1 interaction is only significantly seen in induced MEL cells, suggesting that the interaction between RUNX1 and LSD1 is possibly only needed at terminal differentiation of these cells. We did not analyze the function of LSD1 in the context of RUNX1 any further, because LSD1 also interacts with other members of the GATA1/LDB1/TAL1 complex (Soler et al., unpublished). The interaction of RUNX1 with MYEF2 was picked up by mass spectrometry in non-induced and induced cells, although this interaction is much stronger in noninduced cells. MYEF2 was unknown to play a role in the hematopoietic system since it had only been observed as a suppressor factor in myelinating cells (16). Its role in the hematopoietic system was confirmed by the phenotype observed in the development of the definitive hematopoietic system in zebrafish injected with MO against *Myef2* mRNA. Strikingly, no phenotype could be seen in the development of the primitive hematopoietic system similar to what is observed in *Runx1* knockout mice and zebrafish knockdown studies (21, 29, 33, 50). We conclude that the number of definitive HSC is lower due to improper RUNX1 function via MYEF2.

The genome-wide correlation of RUNX1 ChIP-seq and KD suggests that RUNX1 acts as a repressor and an activator in MEL cells. The complex that would be in part responsible for gene repression is RUNX1-MYEF2. The *in vitro* binding data suggest that RUNX1 and MYEF2 can bind independently from the GATA1 complex, but that they facilitate each others binding. Like the GATA1/TAL1 complex, this complex is important for the repression of a number of erythroid genes in undifferentiated cells. Most RUNX1 target genes show a doubling of expression after the RUNX1 KD, such as *Gata1* and *Cbfa2t3* (Eto2). Others, such as *Ebp4.2*, show a dramatic increase in expression. This suggests that RUNX1 is a repressor of a number of genes in undifferentiated cells but that partners other than MYEF2 (such as Eto2) may also be very important for suppression. It is in fact difficult to determine what the contribution of MYEF2 is to the inhibition of *Ebp4.2* since the MYEF2 KD activates Eto2, which itself is a suppressor of *Ebp4.2*. Thus, two opposite effects are created: the release of suppression by MYEF2 and an increase of suppression by ETO2. This suggests that MYEF2 plays an important role in the maintenance of the correct balance of the quantity of ETO2 prior to terminal differentiation. This would confirm the earlier observation by Goardon et al. (13) that the overexpression of ETO2 leads to an inhibition of differentiation through extended inhibition. In addition, the frequent colocalization suggests that RUNX1 has a role with the GATA1/LDB1/TAL1 complex to suppress the late differentiation program in undifferentiated cells (Table 2; see also Table S3 and Fig. S2 at <http://www.erasmusmc.nl/47738/185891/973174/3784765/mcb2012>). Perhaps most interesting is the regulation of a number of receptors by RUNX1, notably the CSF2RB, IL-9R, and EpoR and the cell cycle regulators p21 and cyclin E. All of these genes show very good binding sites close to or

TABLE 2 Overlap of RUNX1 with GATA1 and TAL1 binding (noninduced) on differentially expressed genes after Runx1 knockdown^a

Binding	Gene status	No. of genes	% overlap
Overlap RUNX1 and GATA1 binding	Upregulated	745	70.70
	Downregulated	553	57.40
Overlap RUNX1 and TAL1 binding	Upregulated	601	57.02
	Downregulated	429	44.55

^a The numbers of genes and the percentages of overlap of the differentially expressed genes are shown.

inside the genes, suggesting that they are direct targets of RUNX1 (e.g., CSF2RB) (see Table S2 at the URL above).

RUNX1 may be even more essential for stress erythropoiesis. For example, ETO2 is important for erythropoiesis *in vitro* (13, 24, 44) and stress erythropoiesis *in vivo* (5). Unfortunately, we were unable to study the role in erythropoiesis of RUNX1 in fetal liver cells due to insufficient KD efficiencies.

In summary, we report here a novel function of the RUNX1 protein in erythroid development. It acts as a repressor of important erythroid genes such as *Cbfa2t3* (Eto2), *Gata1*, and *Ebp4.2*. The repression of these genes is mediated at least in part via MYEF2, which we show to be a novel binding partner of RUNX1. The repressive function of RUNX1 and the complex binding with MYEF2 are lost during differentiation. This suggests that RUNX1 also has a late role in hematopoiesis by keeping erythroid cell-specific genes repressed before terminal differentiation.

ACKNOWLEDGMENTS

We thank Zeliha Ozgur for microarray processing and Mirjam van den Hout for data set handling.

This study was supported by the FP6 Integrated Project EuTRACC, the Stem Cell initiatives SCDD (Netherlands) and NIRM (Netherlands), and the Royal Dutch Academy of Sciences (F.G.).

REFERENCES

- Baldi P, Long AD. 2001. A Bayesian framework for the analysis of microarray expression data: regularized t-test and statistical inferences of gene changes. *Bioinformatics* 17:509–519.
- Beckett D, Kovaleva E, Schatz PJ. 1999. A minimal peptide substrate in biotin holoenzyme synthetase-catalyzed biotinylation. *Protein Sci.* 8:921–929.
- Bravo J, Li Z, Speck NA, Warren AJ. 2001. The leukemia-associated AML1 (Runx1)–CBF β complex functions as a DNA-induced molecular clamp. *Nat. Struct. Biol.* 8:371–378.
- Cantor AB, Orkin SH. 2002. Transcriptional regulation of erythropoiesis: an affair involving multiple partners. *Oncogene* 21:3368–3376.
- Chyla BJ, et al. 2008. Deletion of Mtg16, a target of t(16;21), alters hematopoietic progenitor cell proliferation and lineage allocation. *Mol. Cell. Biol.* 28:6234–6247.
- de Boer E, et al. 2003. Efficient biotinylation and single-step purification of tagged transcription factors in mammalian cells and transgenic mice. *Proc. Natl. Acad. Sci. U. S. A.* 100:7480–7485.
- de Bruijn MF, Speck NA. 2004. Core-binding factors in hematopoiesis and immune function. *Oncogene* 23:4238–4248.
- Dunn C, O'Dowd A, Randall RE. 1999. Fine mapping of the binding sites of monoclonal antibodies raised against the Pk tag. *J. Immunol. Methods* 224:141–150.
- Elagib KE, et al. 2003. RUNX1 and GATA-1 coexpression and cooperation in megakaryocytic differentiation. *Blood* 101:4333–4341.
- Fornieris F, Binda C, Vanoni MA, Mattevi A, Battaglioli E. 2005. Histone

- demethylation catalyzed by LSD1 is a flavin-dependent oxidative process. *FEBS Lett.* 579:2203–2207.
11. Fujiwara T, et al. 2009. Discovering hematopoietic mechanisms through genome-wide analysis of GATA factor chromatin occupancy. *Mol. Cell* 36:667–681.
 12. Garcia-Bassets I, et al. 2007. Histone methylation-dependent mechanisms impose ligand dependency for gene activation by nuclear receptors. *Cell* 128:505–518.
 13. Goardon N, et al. 2006. ETO2 coordinates cellular proliferation and differentiation during erythropoiesis. *EMBO J.* 25:357–366.
 14. Goldfarb AN. 2009. Megakaryocytic programming by a transcriptional regulatory loop: a circle connecting RUNX1, GATA-1, and P-TEFb. *J. Cell. Biochem.* 107:377–382.
 15. Growney JD, et al. 2005. Loss of Runx1 perturbs adult hematopoiesis and is associated with a myeloproliferative phenotype. *Blood* 106:494–504.
 16. Haas S, Stepkowski A, Siracusa LD, Amini S, Khalili K. 1995. Identification of a sequence-specific single-stranded DNA binding protein that suppresses transcription of the mouse myelin basic protein gene. *J. Biol. Chem.* 270:12503–12510.
 17. Hu X, et al. 2009. LSD1-mediated epigenetic modification is required for TAL1 function and hematopoiesis. *Proc. Natl. Acad. Sci. U. S. A.* 106:10141–10146.
 18. Hu Z, et al. 2011. RUNX1 regulates corepressor interactions of PU.1. *Blood* 117:6498–6508.
 19. Huber W, von Heydebreck A, Sultmann H, Poustka A, Vingron M. 2002. Variance stabilization applied to microarray data calibration and to the quantification of differential expression. *Bioinformatics* 18(Suppl 1):S96–S104.
 20. Jowett T, Yan YL. 1996. Double fluorescent in situ hybridization to zebrafish embryos. *Trends Genet.* 12:387–389.
 21. Kalev-Zylinska ML, et al. 2002. Runx1 is required for zebrafish blood and vessel development and expression of a human RUNX1-CBF2T1 transgene advances a model for studies of leukemogenesis. *Development* 129:2015–2030.
 22. Kimmel CB, Ballard WW, Kimmel SR, Ullmann B, Schilling TF. 1995. Stages of embryonic development of the zebrafish. *Dev. Dynam.* 203:253–310.
 23. Kolodziej KE, et al. 2009. Optimal use of tandem biotin and V5 tags in ChIP assays. *BMC Mol. Biol.* 10:6. doi:10.1186/1471-2199-10-6.
 24. Meier N, et al. 2006. Novel binding partners of Ldb1 are required for hematopoietic development. *Development* 133:4913–4923.
 25. Metzger E, et al. 2005. LSD1 demethylates repressive histone marks to promote androgen-receptor-dependent transcription. *Nature* 437:436–439.
 26. Monteiro R, Pouget C, Patient R. 2011. The *gata1/pu.1* lineage fate paradigm varies between blood populations and is modulated by *tif1γ*. *EMBO J.* 30:1093–1103.
 27. Muralidharan V, et al. 1997. Evidence for inhibition of MyEF-2 binding to MBP promoter by MEF-1/Purα. *J. Cell. Biochem.* 66:524–531.
 28. Nishimura S, et al. 2000. A GATA box in the GATA-1 gene hematopoietic enhancer is a critical element in the network of GATA factors and sites that regulate this gene. *Mol. Cell. Biol.* 20:713–723.
 29. North T, et al. 1999. Cbfa2 is required for the formation of intra-aortic hematopoietic clusters. *Development* 126:2563–2575.
 30. Nottingham WT, et al. 2007. Runx1-mediated hematopoietic stem-cell emergence is controlled by a Gata/Ets/SCL-regulated enhancer. *Blood* 110:4188–4197.
 31. Ogawa E, et al. 1993. Molecular cloning and characterization of PEBP2β, the heterodimeric partner of a novel *Drosophila* runt-related DNA binding protein PEBP2α. *Virology* 194:314–331.
 32. Ogawa E, et al. 1993. PEBP2/PEA2 represents a family of transcription factors homologous to the products of the *Drosophila* runt gene and the human AML1 gene. *Proc. Natl. Acad. Sci. U. S. A.* 90:6859–6863.
 33. Okuda T, van Deursen J, Hiebert SW, Grosveld G, Downing JR. 1996. AML1, the target of multiple chromosomal translocations in human leukemia, is essential for normal fetal liver hematopoiesis. *Cell* 84:321–330.
 34. Onodera K, et al. 1997. GATA-1 transcription is controlled by distinct regulatory mechanisms during primitive and definitive erythropoiesis. *Proc. Natl. Acad. Sci. U. S. A.* 94:4487–4492.
 35. Pencovich N, Jaschek R, Tanay A, Groner Y. 2011. Dynamic combinatorial interactions of RUNX1 and cooperating partners regulates megakaryocytic differentiation in cell line models. *Blood* 117:e1–e14.
 36. Putz G, Rosner A, Nuesslein I, Schmitz N, Buchholz F. 2006. AML1 deletion in adult mice causes splenomegaly and lymphomas. *Oncogene* 25:929–939.
 37. Rodriguez P, et al. 2006. Isolation of transcription factor complexes by in vivo biotinylation tagging and direct binding to streptavidin beads. *Methods Mol. Biol.* 338:305–323.
 38. Saleque S, Kim J, Rooke HM, Orkin SH. 2007. Epigenetic regulation of hematopoietic differentiation by Gfi-1 and Gfi-1b is mediated by the cofactors CoREST and LSD1. *Mol. Cell* 27:562–572.
 39. Sasaki K, et al. 1996. Absence of fetal liver hematopoiesis in mice deficient in transcriptional coactivator core binding factor beta. *Proc. Natl. Acad. Sci. U. S. A.* 93:12359–12363.
 40. Satchwell TJ, Shoemark DK, Sessions RB, Toye AM. 2009. Protein 4.2: a complex linker. *Blood Cells Molecules Dis.* 42:201–210.
 41. Satoh Y, et al. 2008. AML1/RUNX1 works as a negative regulator of c-Mpl in hematopoietic stem cells. *J. Biol. Chem.* 283:30045–30056.
 42. Shi Y, et al. 2004. Histone demethylation mediated by the nuclear amine oxidase homolog LSD1. *Cell* 119:941–953.
 43. Soler E, et al. 2011. A systems approach to analyze transcription factors in mammalian cells. *Methods* 53:151–162.
 44. Soler E, et al. 2010. The genome-wide dynamics of the binding of Ldb1 complexes during erythroid differentiation. *Genes Dev.* 24:277–289.
 45. Stadhouders R, et al. 2012. Dynamic long-range chromatin interactions control Myb proto-oncogene transcription during erythroid development. *EMBO J.* 31:986–999.
 46. Takahashi S, et al. 2000. GATA factor transgenes under GATA-1 locus control rescue germline GATA-1 mutant deficiencies. *Blood* 96:910–916.
 47. Tijssen MR, et al. 2011. Genome-wide analysis of simultaneous GATA1/2, RUNX1, FLI1, and SCL binding in megakaryocytes identifies hematopoietic regulators. *Dev. Cell* 20:597–609.
 48. Tracey WD, Jr, Pepling ME, Horb ME, Thomsen GH, Gergen JP. 1998. A *Xenopus* homologue of *aml-1* reveals unexpected patterning mechanisms leading to the formation of embryonic blood. *Development* 125:1371–1380.
 49. Wang JH, et al. 1996. Selective defects in the development of the fetal and adult lymphoid system in mice with an Ikaros null mutation. *Immunity* 5:537–549.
 50. Wang Q, et al. 1996. Disruption of the *Cbfa2* gene causes necrosis and hemorrhaging in the central nervous system and blocks definitive hematopoiesis. *Proc. Natl. Acad. Sci. U. S. A.* 93:3444–3449.
 51. Wang Q, et al. 1996. The CBFβ subunit is essential for CBFα2 (AML1) function in vivo. *Cell* 87:697–708.
 52. Westerfield M. 1995. The zebrafish book. University of Oregon, Eugene, OR.
 53. Willett CE, Cherry JJ, Steiner LA. 1997. Characterization and expression of the recombination activating genes (*rag1* and *rag2*) of zebrafish. *Immunogenetics* 45:394–404.
 54. Wilson NK, et al. 2010. Combinatorial transcriptional control in blood stem/progenitor cells: genome-wide analysis of ten major transcriptional regulators. *Cell Stem Cell* 7:532–544.
 55. Wissmann M, et al. 2007. Cooperative demethylation by JMJD2C and LSD1 promotes androgen receptor-dependent gene expression. *Nat. Cell Biol.* 9:347–353.
 56. Xu G, et al. 2006. Physical association of the patient-specific GATA1 mutants with RUNX1 in acute megakaryoblastic leukemia accompanying Down syndrome. *Leukemia (United Kingdom)* 20:1002–1008.
 57. Yokomizo T, et al. 2008. Runx1 is involved in primitive erythropoiesis in the mouse. *Blood* 111:4075–4080.